Neutronic analyses of the FREYA experiments in support of the ALFRED LFR core design and licensing

Sarotto, M.; Firpo, G.; Kochetkov, A.; Krása, A.; Fridman, E.; Cetnar, J.; Domanska, G.;

Originally published:

June 2019

Journal of Nuclear Engineering and Radiation Science 6(2020)1, 011402

DOI: https://doi.org/10.1115/1.4044000

Perma-Link to Publication Repository of HZDR:

https://www.hzdr.de/publications/Publ-28219

Neutronic analyses of the FREYA experiments in support of the ALFRED LFR core design and licensing

Massimo Sarotto
ENEA - Italian National Agency for New Technologies, Energy and Sustainable Economic Development, Strada per Crescentino 41, 13040 Saluggia, Italy.
e-mail: massimo.sarotto@enea.it

Gabriele Firpo
Ansaldo Nucleare, Corso F.M. Perrone, 25, 16152 Genova, Italy.
e-mail: gabriele.firpo@ann.ansaldoenergia.com

Anatoly Kochetkov
SCK•CEN, Belgian Nuclear Research Centre, Boeretang 200, 2400 Mol, Belgium.
e-mail: anatoly.kochetkov@sckcen.be

Antonin Krása
SCK•CEN, Belgian Nuclear Research Centre, Boeretang 200, 2400 Mol, Belgium.
e-mail: antonin.krasa@sckcen.be

Emil Fridman
HZDR, Helmholtz-Zentrum Dresden-Rossendorf, Bautzner Landstraße 400, 01328 Dresden, Germany.
e-mail: e.fridman@hzdr.de

Jerzy Cetnar
AGH, Faculty of physics and applied computer science, al. Mickiewicza 30, PL-30059 Krakow, Poland.
e-mail: cetnar@newton.fis.agh.edu.pl

Grazyna Domanska
AGH, Faculty of physics and applied computer science, al. Mickiewicza 30, PL-30059 Krakow, Poland.
e-mail: domanska@agh.edu.pl

ABSTRACT

During the EURATOM FP7 project FREYA, a number of experiments were performed in a critical core assembled in the VENUS-F zero-power reactor able to reproduce the ALFRED lead-cooled fast reactor

spectrum in a dedicated island. The experiments dealt with the measurements of integral and local neutronic parameters, such as: the core criticality, the control rod and the lead void reactivity worth, the axial distributions of fission rates for the nuclides of major interest in a fast spectrum, the spectral indices of important actinides (^{238}U, ^{239}Pu, ^{237}Np) respect to ^{235}U. With the main aim to validate the neutronic codes adopted for the ALFRED core design, the VENUS-F core and its characterization measurements were simulated with both deterministic (ERANOS) and stochastic (MCNP, SERPENT) codes, by adopting different nuclear data libraries (JEFF, ENDF/B, JENDL, TENDL).

This paper summarizes the main results obtained by highlighting a general agreement between measurements and simulations, with few discrepancies for some parameters that are here discussed. Additionally, a sensitivity and uncertainty analysis was performed with deterministic methods for the core reactivity: it clearly indicates that the small over-criticality estimated by the different codes/libraries resulted to be lower than the uncertainties due to nuclear data.

1 INTRODUCTION

In the 7th Framework Programme (FP7) of the EURopean ATOMic energy community (EURATOM), the European Commission co-founded the Fast Reactor Experiments for hYbrid Applications (FREYA) collaborative project. The project - carried out between 2011 and 2016 - was launched to support the design and licensing of sub-critical (*i.e.*, accelerator driven) and critical lead-cooled fast spectrum systems, which could be used for the transmutation of minor actinides (Am, Np, Cm nuclides) needed for the closure of the fuel cycle and, hence, for the sustainability of nuclear energy. FREYA was coordinated by the Belgian Nuclear Research Centre (SCK•CEN), where it is available the Vulcan Experimental NUclear Study – Fast (VENUS-F) facility: a zero-power reactor - that can operate in both critical and sub-critical modes - containing core

components and surrounding structures in solid lead in order to simulate lead-cooled systems [1].

This work is focused on the activities performed in the Work Package n. 4 (WP4) devoted to support the development of the Lead-cooled Fast Reactor (LFR), one of the six reactor concepts contemplated within the Generation IV initiative [2]. The availability of experimental data and detailed information on the VENUS-F experimental setups provided measurements suitable for the validation of neutronic codes in a lead environment. The LFR concept chosen as reference is the Advanced Lead-cooled Fast Reactor European Demonstrator (ALFRED):

- that is foreseen in the Strategic Research Agenda of the European Sustainable Nuclear Industrial Initiative [3];
- whose preliminary design was conceived in the EURATOM F7 project LEADER [4] and currently is being carried on by the Fostering ALfred CONstruction (FALCON) international consortium [5].

The present article describes in some details:

- the neutronic codes used in a first stage for the design of the VENUS-F core representative of ALFRED and, successively, for the simulation and analyses of the measurements. The project partners adopted both stochastic and deterministic methods with different nuclear data libraries (§2);
- a brief description of the main features of the VENUS-F reactor and core (§3);
- the rationale adopted for the definition of the VENUS-F critical core layout representative of ALFRED, assembled and characterized within the WP4 (§4);

- the core characterization measurements performed and their comparison with the corresponding neutronic simulations, in order to benchmark the calculation results with the experimental data. The measures dealt with both local and integral parameters, such as: the core criticality (§5.1), the Control Rods (CRs) reactivity worth (§5.2), the axial distributions of fission rates for the fissile and fertile nuclides of major interest in a fast spectrum (§5.3), the spectral indices of important actinides (^{238}U, ^{239}Pu, ^{237}Np) respect to ^{235}U (§5.4) and the lead void reactivity worth to simulate the coolant voiding (§5.5);
- the sensitivity and uncertainty analyses for the core reactivity carried out with deterministic methods (§6);
- the major conclusions that can be drawn from the present work, mainly for what concerns the neutronic codes (and related libraries) validation (§7).

2 THE NEUTRONIC MODELS, CODES AND LIBRARIES

The neutronic models adopted were based on a very detailed description of the VENUS-F facility provided by SCK•CEN to the other FREYA partners: therefore, their applicability for the simulation and characterization of the experiments was accurately verified. As mentioned in §1, the neutronic analyses were performed with both deterministic (ERANOS, §2.1) and stochastic codes (MCNP and SERPENT, §2.2).

2.1 The ERANOS deterministic code

The deterministic neutronic analyses were carried out with the European Reactor ANalysis Optimised calculation System (ERANOS) version 2.2n [6]. It is a modular system and consists of data libraries, deterministic codes and calculation procedures: the different modules perform several functions to analyze reactivity, fluxes, burn-up, reaction rates, etc. of a nuclear system that can be modelled by 1D, 2D and 3D geometries.

The macroscopic cross-sections representing the different zones of the VENUS-F reactor (*e.g.,* core assemblies and lead reflector) were obtained by means of the European Cell Code (ECCO) [7]. An accurate 2D geometry description was adopted for the different components of the core assemblies, while the axial leakages were taken into account by tuning opportunely the buckling value, *e.g.*, for the fissile zone of the FA cell lattice the value chosen in ECCO yields a unitary multiplication factor (k_{eff}) in order to reproduce the critical core conditions. The cross-sections were produced by means of a 1968 energy-group-structure and then condensed in an optimized structure at 49 groups, specifically developed for the VENUS-F experiments. In the sensitivity and uncertainty studies (§6), the cross-sections were condensed in a 33 and 15 energy-group-structure, respectively, available in the ERANOS environment for this kind of analyses. The upper energy limits of the three structures are reported in Table 1: it appears evident that the optimized structure at 49 groups is more refined in the fast part of the spectrum than the “standard” one at 33 groups [7].

The full-core calculations were performed with the TGV module [8], in which the variational nodal method [9, 10] is used to solve the transport equation in a XYZ

geometry model of the whole reactor. The analyses were carried out by adopting the JEFF-3.1 [11] and the ENDF/B-VI.8 [12] nuclear data available in the ECCO-ERANOS environment.

2.2 The MCNP and SERPENT stochastic codes

The stochastic neutronic analyses were carried out with:

- the Monte Carlo N-Particle transport code (MCNP) in two different versions: MCNP5 [13] and MCNP6.1 [14];
- the multi-purpose transport code SERPENT [15].

The MCNP code was used at SCK•CEN as the main tool for design, characterization and safety calculations of the VENUS-F core layouts assembled and characterized during the whole FREYA project. The SERPENT and ERANOS (§2.1) core/reactor models were based on the very detailed MCNP description of the VENUS-F facility, in order to verify their applicability for the simulation and characterization of the experiments.

As MCNP, SERPENT is a three-dimensional continuous-energy Monte Carlo particle transport code - being developed for reactor physics applications including criticality calculations, burnup and decay analyses - that utilizes continues energy ACE-formatted cross section libraries. The main difference between them is that SERPENT adopts [15]:

- the Woodcock delta-tracking method in combination with a typical surface-to-surface ray-tracing in a neutron tracking routine;
- a unionized energy grid for all point-wise reaction cross sections.

The SERPENT and MCNP5 simulations were performed by adopting the JEFF-3.1 nuclear data [11]. Otherwise, the MCNP6.1 calculations were carried out with five different

libraries: JEFF-3.1.1 [16], JEFF-3.2 [17], ENDF/B-VII.1 [18], TENDL-2014 [19] and JENDL-4.0 [20].

3 MAIN FEATURES OF THE VENUS-F CORE

The VENUS facility was built at SCK•CEN in Mol (Belgium) as a zero-power water-moderated thermal critical reactor and it was critical for the first time in 1964. Starting from 2007, due to the increasing interest in Europe for the accelerator driven systems cooled by lead or lead-bismuth eutectic, the VENUS thermal facility was converted into the VENUS-F fast one by installing core components, radial and axial reflectors in solid lead [1].

The cylindrical reactor vessel hosts the core layout made of 12×12 square assembly positions with a lattice pitch of about 8 cm. Fig. 1 shows an horizontal and a vertical view of the layout called Critical Core n. 5 (CC5), that was the “simplest” critical configuration defined, measured and characterized during the FREYA WP3 activities dedicated to the MYRRHA critical reactor concept [21]. The CC5 layout represented also the starting point for the WP4 activities and its main features can be summarized as follows.

- The active core (red, see left frame of Fig. 1) is radially surrounded by Lead Assemblies (LAs, blue), a square Stainless Steel (SS) casing (yellow) and the lead reflector (here not shown).
- The Fuel Assembly (FA) is a 5x5 square matrix (see central frame of Fig. 1) surrounded by a SS-Pb box and filled with U metallic rods (enriched at 30 wt.% in

^{235}U), lead blocks (simulating the coolant in LFR systems) and Aluminum Oxide (Al_2O_3) rods. The latter were introduced to soften the neutron spectrum since the Mixed OXide (MOX) fuel is foreseen in both MYRRHA [22] and ALFRED [4] reactors.

- Two FAs in the CC5 layout are Experimental FAs (EFA-1 and EFA-2, see central frame of Fig. 1) in which an U rod of a standard FA is replaced by a SS guide tube for the insertion of small fission chambers.
- For the reactor control and scram, the core is equipped with six fuel follower Safety Rods (SRs, orange) and two CRs (green): in both systems, the absorbing parts are made by Boron Carbide (B_4C). The CRs are positioned at the fissile core boundary and are used for the fine tuning of the core reactivity during operation. By including SRs and EFAs, the total amount of fissile assemblies results 41.
- A POwder AbsorbeR (POAR) rod (brown) was foreseen on the left side of the core. It is made of pressed B_4C powder and enables a rapid and small insertion of reactivity - about 200 per cent mille (pcm) - in order to apply the rod drop method for reactivity measurements [23].
- As shown in the right frame of Fig. 1 - where a partially inserted CR is depicted - in the axial direction the fissile zone (60 cm height) is embedded by lower and top plates in SS and lead reflectors.

4 THE VENUS-F CORE LAYOUT REPRESENTATIVE OF ALFRED

4.1 Rationale

When addressing the core design - and in perspective the licensing - of a new reactor concept as the LFR, a thorough validation of neutronic calculation codes (and data libraries) is deemed necessary to prove, to the largest extent, the validity of the results and the appropriateness of the design methodologies and tools. The VENUS-F reactor represented an opportunity to perform integral tests and local measurements of the LFR representative neutronic parameters, in order to support the validation of both deterministic and Monte Carlo neutron transport codes. The most aimed requirement for this validation process is the achievement of an "LFR representative spectrum" for the main integral and local neutronic parameters under study.

As mentioned in §1, the LFR concept chosen as reference in the FREYA WP4 is the 300 MW_{th} ALFRED reactor. Fig. 2 depicts the ALFRED core made of hexagonal wrapped FAs having 127 MOX fuel pins each: for power distribution flattening, the core is divided in two radial zones (inner and outer) having the 21.8 and 27.9 Pu wt.% enrichment [4].

4.2 Preliminary spectra analyses

A preliminary study was performed - with the ERANOS deterministic code and the JEFF3.1 nuclear data library (§2.1) - to verify whether the VENUS-F CC5 core could reproduce an LFR representative neutron spectrum. Fig. 3 shows the neutron spectra evaluated in:

- the CC5 layout in the EFA-2 position at core mid-plane (see Fig. 1);
- the ALFRED inner and outer FAs (see Fig. 2).

The comparison - represented by a semi-logarithmic scale - is focused on the fast part of the neutron spectrum above 1 keV[a] through the normalized fluxes per unit lethargy (with 49 energy groups, §2.1). It appears evident that, in spite of the presence of moderating Al_2O_3 rods among the U metal fuel pins (Fig. 1), the CC5 spectrum is still much harder than the ALFRED MOX ones.

4.3 Definition of the CC6 layout

Therefore, a detailed study was performed in order to reproduce, at least locally, a "softer" spectrum closer to the LFR one [24]. The strategy foresaw the insertion of moderating assemblies made only by Al_2O_3 rods (see left frame of Fig. 4) called Alfred Inert Assemblies (AIAs). They were introduced as a chess around the EFA-2 position by creating a 3x3 ALFRED island (see right frame of Fig. 4), able to reproduce an LFR representative spectrum in EFA-2. The resulting VENUS-F core layout - named CC6 - is shown in Fig. 5, where the 3x3 ALFRED island is surrounded by a black dashed line.

4.4 ALFRED representativeness of the CC6 layout

Fig. 6 compares the aimed ALFRED (inner and outer FA) spectra above 1 keV (evaluated with ERANOS/JEFF-3.1) with the spectrum at core mid-plane in the EFA-2 position of the CC6 layout (calculated with MCNP6.1/JEFF-3.2 and ERANOS/JEFF-3.1). It can be noticed the optimal agreement between deterministic and Monte Carlo results and, mostly, at

[a] The lower energy limit used for fast spectra analyses depends on the application (*e.g.*, materials damage, actinides transmutation performances, *etc.*) and usually ranges from 0.1 to 1 MeV: 1 keV is therefore a conservative threshold.

which extent the spectrum obtained in EFA-2 reproduces properly the aimed ALFRED ones.

In order to further verify the ALFRED spectral representativeness of the CC6 layout - and to quantify the improvement in comparison with the CC5 one - an additional study was carried out by calculating the spectral indices in the EFA-2 position for both cores and by comparing them with the aimed ALFRED ones. These indices can be measured through the ratio between count rates obtained by fission chambers of different actinides, thus providing serviceable information about the neutron energy spectrum thanks to the different cross-section behaviors of the nuclides.

The spectral indices of main interest in a fast spectrum were considered, by calculating the ratios between the fission rates in ^{238}U, ^{239}Pu, ^{240}Pu and ^{237}Np respect to ^{235}U. The following notation was adopted:

- F25 and F28 are the fission rates of $^{235}_{92}$U and $^{238}_{92}$U;
- F37 is the fission rate of $^{237}_{93}$Np;
- F40 and F49 are the fission rates of $^{240}_{94}$Pu and $^{239}_{94}$Pu.

By using the multi-group approximation the spectral indices can be defined as:

$$SI^{r} = \frac{\Sigma_g \sigma_g^{r} \phi_g}{\Sigma_g \sigma_g^{F25} \phi_g} \quad (1)$$

where:

- "SI^{r}" is the spectral index value for F28/F25, F40/F25, F49/F25 and F37/F25;
- "ϕ_g" is the flux value in each energy group g;
- "σ_g^{F25}" is the ^{235}U fission microscopic cross section value in each energy group g;

- "σ_g^r" is the fission microscopic cross section value for the nuclide of interest (r) in each energy group g.

Table 2 reports the ratio between the indices obtained in the EFA-2 position at the core mid-plane for the CC5 and CC6 layouts respect to the ones in the ALFRED inner and outer FAs (§4.1). The results - obtained with ERANOS by adopting the 49 energy-group-structure (§2.1) - clearly indicate the better representativeness of the CC6 layout for ALFRED in comparison with the CC5 one. In fact, while the ratio concerning the F49/F25 index did not show a significant improvement (for the ^{239}Pu cross-section behavior fissioning at low energies), the other indices in the CC6 layout resulted to be very close to the ALFRED ones, especially for the outer FA. Most of these indices were effectively measured in the EFA-2 position of the CC6 layout and the results shown in §5.4 demonstrated the accuracy of calculations.

5 EXPERIMENTAL AND CALCULATION RESULTS COMPARISON

The results of the measurements carried out in the VENUS-F CC6 layout (Fig. 5) during the FREYA WP4 activities are collected in [25]. In the following sections, the main outcomes of the neutronic simulations - carried out by the ENEA, Ansaldo Nucleare, HZDR and AGH FREYA partners - are reported for the integral and local parameters measured.

The accuracy of the calculation results - obtained with different codes/libraries (§2) - are expressed in terms of the Calculated-to-Experimental ratio (C/E), by the exception of the axial traverses of fission rates, where both measured and calculated values were

normalized (§5.3). Besides the C/E values, the results concerning the CRs reactivity worth (§5.2), the spectral indices (§5.4) and the lead void reactivity worth (§5.5) are also expressed through the comparison between the Calculation-minus-Experiment (C-E) value and the measurement uncertainty at the 1÷3 σ level.

5.1 Core criticality

Table 3 summarizes the C/E values for the k_{eff} parameter obtained by simulating the CC6 layout with the CRs (axial) position yielding the criticality. A systematic overestimation in the ≅400÷1000 pcm range was obtained with the different codes/libraries, while the statistical uncertainty of the MCNP and SERPENT results is on the order of 10 pcm or less. It is worth noticing that:

- the smallest discrepancy between the calculation and experiment (~400÷500 pcm over-criticality) was obtained with ERANOS / JEFF-3.1 and MCNP6.1 / JENDL-4.0;
- both the code effect (that can be inferred from the JEFF-3.1 values) and the library effect (that can be inferred from the MCNP6.1 values) present a maximum spread of about 500 pcm. A similar result was obtained for other VENUS-F cores measured and simulated during the FREYA WP3 activities devoted to MYRRHA [21];
- besides the nuclear data uncertainties, the systematic over-estimation of the criticality can be due also to geometrical dimensions of the core components and/or materials specifications and it is currently under investigation. Nevertheless, the analyses reported in §6 point out that the calculation accuracy is quite high, if compared with the uncertainties coming from nuclear data.

5.2 Control rods reactivity worth

The calibration of the CRs was measured with the compensation positive period method [27] and the positive period method just moving both rods together [25]. The slope of the calibration curve (pcm/mm) was almost accurately reproduced by all the codes/libraries; the comparison between the sum of the individual worth and the worth of both CRs inserted pointed out that the shadowing effect is practically absent [26]. The individual CRs worth was calculated with respect to the (theoretical) position having both CRs withdrawn at 600 mm. The C/E values and the compatibility between the C-E values and the 1÷3 σ measurement uncertainty are summarized in Table 4. The CR indicated by "CR1" is the one close to the ALFRED island on the bottom-right corner of the CC6 layout, while "CR2" is the one in the top-left corner (see Fig. 5). It is worth noticing that for both CRs:

- most of the C-E values resulted to be lower than the 3 σ measurement uncertainty, but the calculation results depend significantly on the code and nuclear data adopted;
- most of the C/E values resulted to be lower than one and further analyses are required to determine the main reasons of this systematic discrepancy;
- the highest accuracy seems to be obtained with the ERANOS deterministic code.

5.3 Axial traverses of fission rates

Axial traverse measurements were performed along EFA-2 by adopting fission chambers of ^{235}U, ^{238}U and ^{237}Np nuclides (with ≅1 ÷9 mg mass deposit) that were calibrated in the BR1 reactor at SCK•CEN [28]. The chambers position varied from almost the bottom of the fissile zone up to the top of the reactor: during the movement, the critical CRs height was slightly influenced by the fission chamber and its cable, but the impact on the traverse shape was practically negligible since the height variation was about 1 cm [25] and the CRs were located relatively far from the measurement position (see Fig. 5). Both the calculated and experimental traverse values were normalized to the unity, that is by dividing each value by the maximum one at the core mid-plane (*i.e.*, 300 mm axial quota). As examples of results, Fig. 7 depicts the ^{235}U axial traverses - measured and calculated with the ERANOS code - by indicating the subdivision of the different axial zones in EFA-2 (*i.e.*, fissile, SS plates and Pb reflector). Similarly, Fig. 8 depicts the axial traverses for the ^{238}U and ^{237}Np nuclides. For each traverse, the measurements start from the bottom of the fissile zone (0 mm quota in Figs. 7 and 8), while the calculations were extended also below it by obtaining an almost specular shape respect to the core mid-plane. It is worth noticing that:

- all calculations reproduce faithfully the measurements in correspondence of the fissile zone with a cosine shape like behavior;
- the ^{235}U traverse (Fig. 7) presents two peaks in correspondence of the upper and lower SS plates because of the spectra softening in these zones, while in the ^{238}U and ^{237}Np behaviors (Fig. 8) the peaks are not present for their threshold fission response;

- the ^{235}U and ^{238}U calculation under-estimates systematically the measurements in the upper SS plates and lead reflector, with major differences in correspondence of the ^{235}U peaks in the SS plates: this discrepancy is due to the spectra softening at the core/reflector interface not perfectly reproduced by the code[b]. As remarked in [1], another possible reason for the discrepancies found for ^{235}U fission rates at the core boundary could be the impact of the actual antimony content in the LAs and reflector, that will be further investigated in the near future;
- differently, the ^{237}Np experimental traverse is faithfully reproduced also in the upper SS and Pb regions: evidently, its high-energy fission response resulted to be less sensitive to the spectra softening at the core boundary;
- for each axial traverse, there is an almost perfect agreement between the ERANOS JEFF-3.1 and ENDF/B-VI.8 data (calculated by using a 49 energy-group-structure).

Fig. 9÷10 show the same experimental data for the three nuclides compared with the results obtained by the MCNP6.1 code and three different libraries. Similarly to the ERANOS results:

- a very good agreement can be observed in correspondence of the fissile length (*i.e.*, from 0 to 60 cm) for all the nuclides;
- for the ^{235}U traverse (see Fig. 9), the calculations under-estimate the measured values above 60 cm height in the SS plate (where the major differences appear) and Pb reflector regions;

[b] That is the moderation of fast neutrons – coming from the fissile zone or backscattered from the lead reflector – inside the steel not properly reproduced by calculations.

- the calculations reproduce faithfully the ^{237}Np traverse (see right frame of Fig. 10) – and almost faithfully the ^{238}U one (see left frame of Fig. 10) – along all the measured points (*i.e.*, also in SS and Pb regions). It is worth noticing that, in comparison with the ^{235}U and ^{237}Np nuclides, the ^{238}U fission cross-section resulted to be more sensitive to the library adopted.

Analogous behaviors were found also for the MCNP5/JEFF-3.1 and SERPENT/JEFF-3.1 results [26].

5.4 Spectral indices

The measurement of spectral indices was performed with fission chambers having 20÷200 mg mass deposit of actinides [29]. As defined in (1), the count rates coming from ^{238}U, ^{239}Pu and ^{237}Np chambers were normalized to the count rates of the ^{235}U one. Table 5 reports the C/E values of the indices measured and calculated with different codes/libraries, as well as the comparison between the C-E values and the measurement uncertainty at the 1÷3 σ level. The calculation results were obtained from cells/meshes in EFA-2 centered at the core mid-plane:

- with ERANOS, the indices were evaluated in an axial mesh of ≅5 cm height;
- with the stochastic codes, the indices were obtained in a 6 cm height cylindrical cell.

From the C-E results in Table 5 it can be observed that:

- for the F28/F25 index, the highest accuracy (C-E < 3 σ) seem to be obtained with ERANOS (JEFF-3.1 and ENDF/B-VI.8 libraries) and MCNP6.1 (JEFF-3.2 and TENDL-2014 libraries);

- for the F49/F25 index (that is the less sensitive to the fast spectrum), a very high accuracy (C-E < 1 σ) was obtained for almost all codes/libraries;
- for the F37/F25 index, a quite good accuracy (C-E < 3 σ) was obtained for almost all codes/libraries.

Therefore, the best agreement between measurements and calculations was obtained for the F49/F25 index, while for F37/F25 and F28/F25 it resulted to be slightly worse with the major part of the C/E values lower than one. This general trend seems to indicate that most of the codes/libraries simulate:

- more accurately the fissions occurring in the ^{239}Pu nuclide, that fissions at low energies;
- less accurately the fissions occurring in ^{238}U and ^{237}Np nuclides, having a threshold fission cross-section behavior.

Besides these aspects, a specific issue affected the calculation accuracy of the F28/F25 index. As remarked in [30], a systematic effect was found for a tiny amount of ^{235}U usually present as an impurity in the ^{238}U fission chamber deposit (≅0.36%). Nevertheless, this impurity has an almost negligible effect in fast neutron spectrum media (as the EFA-2 in the CC6 layout), while it resulted more evident when analyzing media with partially thermalized spectra, see *e.g.*, [31].

5.5 Lead void reactivity effects

The reactivity effects due to the coolant density - and eventually voiding - are of a paramount importance for the safety of each nuclear installation. To investigate the

lead void reactivity effect, the lead rods were removed in the FAs belonging to the ALFRED island and replaced with empty SS cans, as shown in the left frame of Fig. 11. As indicated in the right frame of Fig. 11, two cases (A and B) were measured and simulated by voiding - over the 60 cm fissile length - one FA (Case A: where a standard FA replaced the EFA-2) and three FAs (Case B).

Table 6 shows the C/E values - and the C-E values compared with the $1 \div 3\ \sigma$ measurement uncertainty - obtained with different codes/libraries for the core reactivity variations induced by the lead voiding. The results clearly indicate that:

- a very high calculation accuracy (C-E < σ) was obtained with all Monte Carlo codes and libraries for A and B cases;
- the ERANOS code sensibly over-estimates the lead void reactivity effect of 15÷30% (with C-E > 3 σ). This result confirms the difficulties of deterministic codes to simulate this phenomenon: the main causes deal with the simulation of voided media (here modelled with a negligible 10^{-15} g cm^{-3} Pb density) and with the spatial homogenization occurring in the ECCO cell calculations (providing the macroscopic cross-sections for the ERANOS full-core analyses, §2.1).

Additional ERANOS calculations were performed by varying the “void” fraction (with the complement in Pb) in the (one and three) FAs belonging to the ALFRED island: as expected, the core reactivity tends to safely decrease by increasing the void amount with an almost linear behavior [26].

6 SENSITIVITY AND UNCERTAINTY ANALYSES

6.1 Brief summary of background theory and calculation methods

To evaluate the impact of the neutron cross-section uncertainties on the k_{eff} value, a sensitivity study (using the perturbation theory) followed by an uncertainty assessment (using covariance data) were adopted. The sensitivity analysis was based on the adjoin approach, that is implemented in the ERANOS system code [32].

The starting point for these studies is represented by the sensitivity coefficients of the k_{eff} value as a function of a variation of the cross-sections σ:

$$S_k = \frac{\partial k_{eff}}{\partial \sigma} \frac{\sigma}{k_{eff}} \tag{2}$$

Afterwards, the variation of the cross-sections which causes a variation of the Boltzmann operator (here named "*M*") can be evaluated linearly by adopting the standard perturbation theory. In some details, by calculating the direct and adjoin fluxes in the critical system (Φ and Φ^*, respectively):

$$M\Phi = \left(A - \frac{1}{k}F\right)\Phi = 0 \tag{3}$$

$$M^*\Phi^* = \left(A^* - \frac{1}{k}F^*\right)\Phi^* = 0 \tag{4}$$

where "*A*" is the loss (leakage + absorption) operator and "*F*" is the fission production operator, the sensitivity coefficient (2) can be evaluated with:

$$S_k = -\mathrm{k}\frac{\langle \Phi^*, \left(A - \frac{F}{k}\right)\Phi \rangle}{\langle \Phi^*, F\Phi \rangle} \tag{5}$$

where "⟨ , ⟩" denotes the integration over space, angle and energy.

In the present analysis the diffusion approximation was utilized. Consequently, the integration is limited over space and energy: the scalar flux adopted was obtained starting from an original angular flux evaluated by the S8 symmetric discretization and cross-sections calculated at the first order (P1) of the Legendre polynomials.

Nevertheless, the errors introduced by the diffusion approximation are partially compensated by the ratio of the space-energy integrals appearing both at numerator and denominator in (5). Differently from the results reported in §4-5 obtained with a 49 energy-group-structure, the sensitivity evaluations were performed by using the standard structure at 33 energy groups (see Table 1) available in the ERANOS environment for this kind of analysis.

The sensitivity coefficients (5) permit to link the uncertainties on nuclear data with the uncertainty on the k_{eff} value by adopting a dispersion or covariance matrix (B) with the relation:

$$\sigma_k^2 = S_k B S_k^t \tag{6}$$

The integral parameter uncertainties were calculated using relation (6) and the BOLNA covariance matrix, developed through a joint effort of several laboratories (Brookhaven, Oak Ridge, Los Alamos, NRG Petten and Argonne) [33]. The BOLNA matrix was selected because of its availability in the ERANOS environment in a 15-energy-group structure (see Table 1) and for its coherence with the libraries adopted (JEFF-3.1 and ENDF/B-VI.8).

The main results of the sensitivity and uncertainty study carried out for the CC6 layout (Fig. 5) are reported in §6.2 and §6.3, respectively. In both cases it was evaluated the impact of nuclear data and the results show the dependence of the k_{eff} parameter on each energy group and/or each cross-section and/or each isotope considered.

6.2 Main results of sensitivity analysis

The sensitivity analysis was carried out with ERANOS by adopting the JEFF-3.1 and ENDF/B-VI.8 nuclear data. The nuclides considered were: ^{235}U, ^{238}U, ^{56}Fe, ^{206}Pb, ^{207}Pb, ^{208}Pb, ^{50}Cr, ^{52}Cr, ^{53}Cr, ^{54}Cr, Al^{27} and ^{16}O. As examples of results:

- Fig. 12 reports the ERANOS / JEFF-3.1 (left) and ERANOS / ENDF/B-VI.8 (right) values of the sensitivity coefficients per each energy group and per each cross-section, summed over the isotopes considered. The two libraries yield very similar trends (with differences lower than 5% in the energy groups of major interest): the highest values appear for the coefficients related to the fission cross-sections (impacting also on the production term "$\nu \cdot \Sigma_f$") and, mainly, the average number of neutrons emitted per fission (NU $\equiv \nu$ in Figs. 12 and 13) approximately between the 4th and 16th energy group, that corresponds to the 10 keV÷3 MeV range. Also the capture cross-sections yield a significant (negative) contribution.
- Fig. 13 reports the ERANOS / JEFF-3.1 sensitivity coefficients per each isotope considered and per each cross-section, summed over the 33 energy groups (also in this case the ENDF/B-VI.8 values, here not shown, present a very similar trend with differences lower than 2%). The results confirm that the capture and fission cross-sections and the average number of neutrons emitted per fission by ^{235}U and ^{238}U yield the main contributes.

It can be further mentioned that almost all the sensitivity coefficients are positive, with the exception of the capture ones (for most of the energy groups) and the inelastic scattering at higher energies (*i.e.*, firsts energy groups).

6.3 Main results of uncertainty analysis

The uncertainty analysis was carried out with ERANOS by adopting the JEFF3.1 and ENDF/B-VI.8 nuclear data. The results obtained show similar trends and values with the two libraries and for this reason only some of them are here shown. The nuclides considered were: ^{235}U, ^{238}U, ^{56}Fe, ^{206}Pb, ^{207}Pb, ^{208}Pb, ^{52}Cr, ^{27}Al and ^{16}O. As examples of results:

- Table 7 reports the ERANOS / ENDF/B-VI.8 uncertainty on the k_{eff} value - summed over the 15 energy groups, per each isotope and per each cross-section[c] - while Fig. 14 shows them in a graphical form. The highest contribution to the uncertainty is due to the ^{235}U capture term. Significant contributions appear also for the number of neutrons per fissions ν (NU $\equiv \nu$ in Figs. 14 and 15) and fission cross-section of ^{235}U, together with ν, the capture and inelastic cross-sections of ^{238}U.
- Fig. 15 reports the ERANOS/JEFF-3.1 uncertainty on the k_{eff} value summed over the isotopes considered per each energy group and per each cross-section. The highest contribution is due to the capture term approximately between the 4th and 9th energy group, that corresponds to the 10 keV÷1.5 MeV range (see Table 1).
- Fig. 16 shows the ERANOS/JEFF3.1 uncertainty on the k_{eff} value summed over the cross-sections per each isotope considered and per each energy group. The highest contribution is due to the ^{235}U isotope in the energy range approximately between 10 keV and 1.5 MeV. A significant contribution is also due to the ^{238}U isotope at high energies, presumably for the threshold behavior of its fission cross-section.

[c] Being an uncertainty analysis, the total of the row and column values in Table 7 are obtained by the square root of the sum of the square of each term.

The results indicated that, as a whole, cross-sections and ν values yield a total uncertainty of about 2% (2.17 / 2.15% with JEFF-3.1 / ENDF/B-VI.8, respectively), corresponding to a Δk_{eff} of about 2000 pcm.

7 CONCLUDING REMARKS

The experimental campaign carried out in the WP4 of the FREYA EU FP7 project has represented a valuable support for the core design - and in perspective the licensing - of a new reactor concept as ALFRED. The VENUS-F facility provided the opportunity to perform significant validation activities for the neutronic codes and data libraries used for the LFR studies. For this purpose, the ALFRED spectral representativeness was obtained through a dedicated critical core configuration - named CC6 - defined, assembled and characterized experimentally during FREYA. In this layout, the ALFRED MOX spectrum was reproduced faithfully above 1 keV (and hence suitable for the LFR fast spectrum) thanks to the introduction of Al_2O_3 moderating assemblies among the VENUS-F FAs made of U metallic rods.

The most important integral and local neutronic parameters fundamental for the core design were measured. The experiments were designed and simulated by means of both stochastic (MCNP and SERPENT) and deterministic (ERANOS) codes coupled with different neutron data libraries (JEFF, ENDF/B, JENDL, and TENDL). The models used in the analyses simulated accurately the geometry and materials of the whole VENUS-F system, by a detailed representation of the core and surrounding structures, which represent a fundamental aspect of the validation process.

The major remarks that can be drawn from the comparison between the calculation and experimental results can be summarized as follows.

- A systematic over-estimation of the core reactivity in the 0.4÷1% range was found with all the codes/libraries. The main contribution for this discrepancy should come from the nuclear data uncertainties, as deduced from the sensitivity and uncertainty analyses performed with the ERANOS code indicating a uncertainty level of about 2%. As expected, the highest contributions come from the U isotopes (^{235}U capture cross-section; ^{235}U and ^{238}U fission cross-sections and average number of neutrons emitted per fission). Another aspect which may have contributed to the k_{eff} uncertainty is the absence of detailed information about the possible variance of the ^{235}U weight amount in the fuel.
- All the codes / libraries yield quite accurate values for the CRs worth, even if a slight systematic underestimation was found and further analyses are required to identify the main reasons.
- All codes/libraries reproduce faithfully the ^{235}U, ^{238}U and ^{237}Np axial traverses of fission rates measured in the EFA-2 experimental channel in correspondence of the fissile length. Otherwise, some discrepancies appear for the U^{235} and U^{238} traverses in correspondence of the upper SS plates and lead reflector, mainly because of the spectra softening at the core/reflector interface not perfectly reproduced by the codes.
- An agreement within the 1÷3 σ measurement uncertainty was found for the spectral indices measured in EFA-2 (at core mid-plane) - where the ALFRED spectrum is

reproduced - for almost all codes/libraries. The highest accuracy (C-E < 1 σ) was found for the F49/F25 index, while for F28/F25 and F37/F25 it resulted to be lower for the difficulty in simulating the ^{238}U and ^{237}Np threshold fission cross-section behaviors in the high-energy part of the spectrum.

- A very high calculation accuracy (C-E < 1 σ) was obtained by the Monte Carlo codes and libraries for the simulation of the lead void reactivity effect. On the contrary, the ERANOS code yielded a 15÷30% over-estimation (with C-E > 3 σ) by confirming the difficulties of deterministic codes in the modelling of voided regions.

As general remarks about the codes / libraries adopted in the analyses, it can be stated that:

- by the exception of the void effect, the ERANOS deterministic code (coupled with the JEFF3.1 and ENDF/B-VI.8 libraries) provided quite accurate results for every parameter;
- the MCNP and SERPENT stochastic codes provided quite accurate results for almost all parameters, with major discrepancies for the F28/F25 and F37/F25 spectral indices and an accuracy lower than the ERANOS code for the CR worth. While the MCNP5 and SERPENT C/E values are available only with JEFF3.1 data, the analyses pointed out that the most accurate MCNP6.1 results were obtained with the JEFF-3.2 and ENDF/B-VII.1 libraries, by the exception of criticality where the JENDL-4.0 data reproduced the lowest over-estimation of the core reactivity.

Finally, a couple of main conclusions can be drawn from the general agreement between experiments and calculations. First, the code/libraries adopted represented an

efficient and reliable tool for the modelling of the VENUS-F critical core examined and related experiments. As a consequence, the same codes/libraries could be a reliable tool also for the design and in perspective the licensing of the LFRs, by taking into account that the ALFRED spectrum was faithfully reproduced in a dedicated island and not in the whole core.

ACKNOWLEDGMENT

The authors want to acknowledge Drs. M. Carta and G. Grasso (ENEA) for the valuable technical support, the VENUS team (SCK•CEN) for the experimental activity and all the partners of the FREYA project for their fruitful contributions.

The computing resources for the ERANOS simulations were provided by the CRESCO / ENEAGRID High Performance Computing infrastructure and its staff (http://www.cresco.enea.it): the infrastructure is funded by ENEA and by national and European research programs.

FUNDING

The FREYA project was co-founded by the European Commission during the 7th Framework Programme.

NOMENCLATURE

A	loss (leakage + absorption) operator
B	dispersion or covariance matrix
F25, F28	fission rates of $^{235}_{92}\mathrm{U}$ and $^{238}_{92}\mathrm{U}$
F37	fission rates of $^{237}_{93}\mathrm{Np}$
F40, F49	fission rates of $^{240}_{94}\mathrm{Pu}$ and $^{239}_{94}\mathrm{Pu}$
ϕ_g	flux value in each energy group g
ϕ^*	adjoin flux
k_{eff}	multiplication factor
M	Boltzmann operator
SI^r	spectral index value (for F28/F25, F40/F25, F49/F25 and F37/F25)
S_k	sensitivity coefficient for k_{eff}
σ	microscopic cross-section
σ_g^{F25}	^{235}U fission microscopic cross section value in each energy group g
σ_g^r	fission microscopic cross section value for nuclide r in each energy group g
σ_k^2	total uncertainty for k_{eff}

Acronyms and abbreviations

AIA	Alfred Inert Assembly
ALFRED	Advanced Lead-cooled Fast Reactor European Demonstrator
CC	Critical core
C-E	Calculated-minus-Experimental
C/E	Calculated-to-Experimental
CR	Control Rod
ECCO	European Cell COde
EFA	Experimental Fuel Assembly
ERANOS	European Reactor ANalysis Optimised System
EURATOM	EURopean ATOMic energy community
FA	Fuel Assembly
FALCON	Fostering ALfred CONstruction
FREYA	Fast Reactor Experiments for hYbrid Applications
FP	Framework Program
LA	Lead Assembly
LFR	Lead Fast Reactor
MCNP	Monte Carlo N-Particle
MOX	Mixed OXide
pcm	per cent mille

POAR	POwder AbsorbeR
SR	Safety Rod
SS	Stainless Steel
VENUS-F	Vulcan Experimental NUclear Study - Fast
WP	Work Package

REFERENCES

[1] Kochetkov, A., Wagemans, J., Krása, A., Vittiglio, G., Uyttenhove, W., and Hernandez, J., 2016, "The Lead-Based VENUS-F Facility: Status of the FREYA Project", EPJ Web of Conf. **106**, 06004, DOI: https://doi.org/10.1051/epjconf/201610606004.

[2] GIF, 2002, "Generation IV Technology Roadmap", GIF 002-00, https://www.gen-4.org.

[3] ESNII, 2013, "Strategic Research and Innovation Agenda of the European Sustainable Nuclear Industrial Initiative", http://www.snetp.eu

[4] Grasso, G., Petrovich, C., Mattioli, D., Artioli, C., Sciora, P., Gugiu, D., Bandini, G., Bybelis, E., and Mikityuk, M., 2014, "The core design of ALFRED, a demonstrator for the European lead-cooled reactors", J. Nucl. Eng. Des. **278**,pp. 287–301.

[5] FALCON, 2014, "Fostering the ALFRED Construction", https://www.euronuclear.org/e-news/e-news-43/ansaldo.htm

[6] Rimpault, G., Plisson, D., Tommasi, J., Jacqmin, R., and Rieunier, J.M., 2002, "The ERANOS code and data system for Fast Reactor neutronic analyses", Proc. Int. Conf. PHYSOR 2002, New Frontiers of Nuclear Technology: reactor physics, safety and high-performance computing, Seoul (Korea), October 7-10.

[7] Rimpault, G., 1997, "Physics documentation of ERANOS: the ECCO cell code", CEA Tech. Rep. DERSPRC-LEPh-97-001.

[8] Palmiotti, G., Carrico, C.B., and Lewis, E.E., 1991, "Variational Nodal Method for the solution of the diffusion and transport equation in two and three dimensional geometries", CEA Tech. Rep. DRN DER NT-SPRC-LEPh-91-208.

[9] Dilber, I., and Lewis, E.E., 1985, "Variational Nodal Methods for Neutron Transport", J. Nucl. Sc. Eng. **91**, pp. 132-142.

[10] Carrico, C.B., Lewis E.E., and Palmiotti, G., 1992, "Three-dimensional Variational Nodal Transport Methods for Cartesian, Triangular and Hexagonal Criticality Calculations", J. Nucl. Sc. Eng. **111**, pp. 168-179.

[11] Koning, A.J., Forrest, R., Kellett, M., Mills, R., Henriksson, H., and Rugama, Y., 2006, "The JEFF3.1 nuclear data library", OECD/NEA Tech. rep. ISBN 92-64-02314-3, https://www.oecd-nea.org/dbdata/nds_jefreports/jefreport-21/jeff21.pdf

[12] Lemmel, H.D., McLaughlin, P.K., and Pronyaev, V.G., "The U.S. Evaluated Nuclear Data Library for Neutron Reaction Data by the US National Nuclear Data Center, Nuclear

data section, International Atomic Energy Agency, ENDF/B-VI release 8 (Last release of ENDF/B-VI)", Tech. Rep. IAEA-NDS-100, Rev. 11.

[13] X-5 Monte Carlo team, 2003, "MCNP — A General Monte Carlo N-Particle Transport Code, Version 5, Volume II: User's guide", Los Alamos National Laboratory Tech. Rep. LA-CP-03-0245.

[14] Pelowitz, D.B., Ed., 2013, "MCNP6 User's Manual Version 1.0", Los Alamos National Laboratory Tech. Rep. LA-CP-13-00634.

[15] Leppänen, J., Pusa, M., Viitanen, T., Valtavirta, V., and Kaltiaisenaho, T., 2015, "The Serpent Monte Carlo code: Status, development and applications in 2013", J. Ann. Nucl. En. **82**, pp. 142–150.

[16] Santamarina, A., Bernard, D., and Rugama, Y., 2009, "The JEFF-3.1.1 Nuclear Data Library", OECD/NEA Tech. Rep. ISBN 978-92-64-99074-6 (NEA No. 6807).

[17] OECD/NEA Data Bank, 2014, "JEFF-3.2 evaluated data library - Neutron data", http://www.oecd-nea.org/dbforms/data/eva/evatapes/jeff_32/

[18] Obložinský, P., 2011, "Special Issue on ENDF/B-VII.1 library", J. Nuclear Data Sheets **112** Issue 12, pp. 2887-3152.

[19] Koning, A.J., and Rochman, D., 2012, "Modern Nuclear Data Evaluation with the TALYS code system", J. Nuclear Data Sheets **113**, Issue 12, pp. 2841-2934.

[20] Shibata, K., Iwamoto, O., Nakagawa, T., Iwamoto, N. Ichihara, A., Kunieda, S., Chiba, A., Furutaka, K., Otuka, N., Ohsawa, T., Murata, T., Matsunobu, H., Zukeran, A. Kamada, S., and Katapura, J., 2011, "JENDL-4.0: a new library for nuclear science and engineering", J. Nucl. Sc. Tech. **48** (1), pp. 1-30.

[21] Krása, A., Kochetkov, A., Baeten, P., Vittiglio, G., Wagemans, J., and Bécares, V., 2017, "Comparative study on neutron data in integral experiments of MYRRHA mock-up critical cores in the VENUS-F reactor", EPJ Web of Conf. **146**, 06019, DOI: https://doi.org/10.1051/epjconf/201714606019.

[22] Abderrahim, H.A., Baeten, P., De Bruyn D., and Fernandez, R., 2012, "MYRRHA - A Multi-purpose fast spectrum research reactor", J. Energy Conversion and Management **63**, pp. 4-10.

[23] Uyttenhove, W., Baeten, P., Ban, G., Billebaud, A., Chabod, S., Dessagne, P., Kerveno, M., Kochetkov, A., Leouey, J.L., Marie, N., Mellier, F., Steckmeyer, J.C., Thyébault, H.E., Vittiglio, G., and Wagemans, J., 2012, "Experimental Results from the

VENUS-F Critical Reference State for the GUINEVERE Accelerator Driven System Project", J. IEEE Transactions on Nuclear Science **59**(6), pp. 3194–3200.

[24] Sarotto, M., Firpo, G., Kochetkov, A., Krása, A., Vittiglio, G., Wagemans, J., and Fabrizio, V., 2015, "LFR mock-up definition", Deliverable D4.1 EURATOM FP7 FREYA project.

[25] Kochetkov, A., Krása, A., Vittiglio, G., Wagemans, J., Firpo, G., Fabrizio, V., and Sarotto, M., 2015, "LFR mock-up characterization", Deliverable D4.2 EURATOM FP7 FREYA project.

[26] Sarotto, M., Firpo, G., Kochetkov, A., Krása, A., Vittiglio, G., Wagemans, J., Fridman, E., Cetnar, J., Domanska, G., and Fabrizio, V., 2016, "LFR mock-up reactivity effects", Deliverable D4.3 EURATOM FP7 FREYA project.

[27] Misawa, T., Unesaki, H,. and Pyeon, C., 2010, Nuclear Reactor Physics Experiment, Kyoto University press., ISBN 978-4-87698-959-1.

[28] Wagemans, J., Malambu, E., and Borms, L., 2012, "The neutron standard fields at the BR1 reactor at SCK•CEN", J. ASTM International **9**(3), pp. 1–7.

[29] Wagemans, J., Borms, L., Kochetkov, A., Krása, A., Van Grieken, C., and Vittiglio, G., 2018, "Nuclear instrumentation in VENUS-F", EPJ Web of Conferences **170**, 04027, DOI: https://doi.org/10.1051/epjconf/201817004027.

[30] Kochetkov, A., Krása, A., Baeten, P., Vittiglio, G., Wagemans, J., Becares, V., Bianchini, G., Fabrizio, V., Carta, M., Firpo, G., Fridman, E., and Sarotto, M., 2017, "Analysis of C/E results of fission rate ratio measurements in several fast lead VENUS-F cores", EPJ Web of Conferences **146**, 06007, DOI: https://doi.org/10.1051/epjconf/201714606007.

[31] Sarotto, M., Kochetkov, A., Krása, A., Bianchini, G., Fabrizio, V., Carta, M., Peluso, V., Vittiglio, G., and Wagemans, J., 2018, "The neutronic modelling of the VENUS-F critical core experiments with the ERANOS deterministic code (FREYA EU FP7 project)", J. Ann. Nucl. En. **121**, pp. 626-637.

[32] Tommasi, J., 2006, "Standard perturbation theory and applications", ERANOS users' workshop, Cadarache (F), May 29-June 2.

[33] Salvatores, M., and Jacqmin, R., 2008, "Uncertainty and target accuracy assessment for innovative systems using recent covariance data evaluations (International Evaluation Co-operation Volume 26)", OECD/NEA Tech. Rep. WPEC-26 ISBN 978-92-64-99053-1.

Figure Captions List

Fig. 1 The VENUS-F CC5 layout (left frame), the standard FA and the EFA (central frame), an axial view of some FAs with a partially inserted CR (right frame)

Fig. 2 The ALFRED LFR core layout (1/4 symmetry, left frame) and FA design (right frame)

Fig. 3 Comparison between neutron spectra calculated in the CC5 layout (EFA-2 position, core mid-plane) and in the ALFRED inner and outer FAs (ERANOS/JEFF-3.1, semi-logarithmic scale)

Fig. 4 The AIA (left frame, made of 25 Al_2O_3 rods) and the 3x3 ALFRED island (right frame) made of: 4 AIAs, 2 standard FAs, 2 LAs and the EFA-2 in the center

Fig. 5 The VENUS-F CC6 layout representative of ALFRED made of: 33 FAs, 6 fuel follower SRs, 2 EFAs, 4 AIAs, 2 CRs, 1 POAR rod, the surrounding LAs and SS casing

Fig. 6 Calculated spectra in the CC6 layout (EFA-2 position, core mid-plane) compared with the ALFRED FA ones (ERANOS/JEFF-3.1 and MCNP6.1/JEFF-3.2; semi-logarithmic scale)

Fig. 7 Experimental and ERANOS (JEFF-3.1 and ENDF/B-VI.8) axial traverses in EFA-2 for U^{235} fission rates (normalized to 1 at core mid-plane)

Table Caption List

Table 1Upper limits of the 15, 33 and 49 energy-group structures adopted in ERANOS calculations

15 energy groups		33 energy groups		49 energy groups	
Group	E (MeV)	Group	E (MeV)	Group	E (MeV)
1	$1.9640\ 10^{1}$	1	$1.9640\ 10^{1}$	1	$1.9640\ 10^{1}$
				2	$1.7333\ 10^{1}$
				3	$1.4918\ 10^{1}$
				4	$1.3840\ 10^{1}$
				5	$1.1618\ 10^{1}$
		2	$1.0000\ 10^{1}$	6	$1.0000\ 10^{1}$
				7	$8.1873\ 10^{0}$
				8	$6.7032\ 10^{0}$
2	$6.0653\ 10^{0}$	3	$6.0653\ 10^{0}$	9	$6.0653\ 10^{0}$
				10	$5.4881\ 10^{0}$
				11	$4.4933\ 10^{0}$
		4	$3.6788\ 10^{0}$	12	$3.6788\ 10^{0}$
				13	$3.0119\ 10^{0}$
				14	$2.4660\ 10^{0}$
3	$2.2313\ 10^{0}$	5	$2.2313\ 10^{0}$	15	$2.2313\ 10^{0}$
				16	$2.0190\ 10^{0}$
				17	$1.6530\ 10^{0}$
4	$1.3534\ 10^{0}$	6	$1.3534\ 10^{0}$	18	$1.3534\ 10^{0}$
				19	$1.2246\ 10^{0}$
				20	$1.1080\ 10^{0}$
				21	$1.0026\ 10^{0}$
				22	$9.0718\ 10^{-1}$
		7	$8.2085\ 10^{-1}$	23	$8.2085\ 10^{-1}$
5	$4.9787\ 10^{-1}$	8	$4.9787\ 10^{-1}$	24	$4.9787\ 10^{-1}$
		9	$3.0197\ 10^{-1}$	25	$3.0197\ 10^{-1}$
6	$1.8316\ 10^{-1}$	10	$1.8316\ 10^{-1}$	26	$1.8316\ 10^{-1}$
		11	$1.1109\ 10^{-1}$	27	$1.1109\ 10^{-1}$
7	$6.7380\ 10^{-2}$	12	$6.7380\ 10^{-2}$	28	$6.7380\ 10^{-2}$
		13	$4.0868\ 10^{-2}$	29	$4.0868\ 10^{-2}$
8	$2.4788\ 10^{-2}$	14	$2.4788\ 10^{-2}$	30	$2.4788\ 10^{-2}$
		15	$1.5034\ 10^{-2}$	31	$1.5034\ 10^{-2}$
9	$9.1188\ 10^{-3}$	16	$9.1188\ 10^{-3}$	32	$9.1188\ 10^{-3}$
		17	$5.5308\ 10^{-3}$	33	$5.5308\ 10^{-3}$
		18	$3.3546\ 10^{-3}$	34	$3.3546\ 10^{-3}$
10	$2.0347\ 10^{-3}$	19	$2.0347\ 10^{-3}$	35	$2.0347\ 10^{-3}$
		20	$1.2341\ 10^{-3}$	36	$1.2341\ 10^{-3}$

		21	$7.4852\ 10^{-4}$	37	$7.4852\ 10^{-4}$
11	$4.5400\ 10^{-4}$	22	$4.5400\ 10^{-4}$	38	$4.5400\ 10^{-4}$
		23	$3.0433\ 10^{-4}$	39	$3.0433\ 10^{-4}$
		24	$1.4863\ 10^{-4}$	40	$1.4863\ 10^{-4}$
		25	$9.1661\ 10^{-5}$	41	$9.1661\ 10^{-5}$
		26	$6.7904\ 10^{-5}$	42	$6.7904\ 10^{-5}$
		27	$4.0169\ 10^{-5}$	43	$4.0169\ 10^{-5}$
12	$2.2603\ 10^{-5}$	28	$2.2603\ 10^{-5}$	44	$2.2603\ 10^{-5}$
		29	$1.3710\ 10^{-5}$	45	$1.3710\ 10^{-5}$
		30	$8.3153\ 10^{-6}$	46	$8.3153\ 10^{-6}$
13	$4.0000\ 10^{-6}$	31	$4.0000\ 10^{-6}$	47	$4.0000\ 10^{-6}$
14	$5.4000\ 10^{-7}$	32	$5.4000\ 10^{-7}$	48	$5.4000\ 10^{-7}$
15	$1.0000\ 10^{-7}$	33	$1.0000\ 10^{-7}$	49	$1.0000\ 10^{-7}$

Table 2 Ratio between the spectral indices calculated in the EFA-2 position of the CC5 and CC6 layouts respect to the ALFRED inner and outer FA ones (ERANOS)

Core	ALFRED FA	Library	F28/F25	F49/F25	F37/F25	F40/F25
CC5	Inner	JEFF-3.1	2.048	1.199	1.983	1.795
	Outer	JEFF-3.1	1.536	1.199	1.488	1.508
CC6	Inner	JEFF-3.1	1.416	1.073	1.307	1.262
		ENDF/B-VI.8	1.448	1.071	1.289	
	Outer	JEFF-3.1	1.062	1.073	0.980	1.060
		ENDF/B-VI.8	1.086	1.071	0.967	

Table 3C/E values for the k_{eff} parameter obtained with different codes/libraries in the CC6 layout.

Code	Library	C/E
MCNP5	JEFF-3.1	1.009
SERPENT		1.008
ERANOS		1.004
	ENDF/B-VI.8	1.010
MCNP6.1	JEFF-3.1.1	1.008
	JEFF-3.2	1.010
	ENDF/B-VII.1	1.008
	TENDL-2014	1.008
	JENDL-4.0	1.005

Table 4C/E and C-E values for the CRs reactivity worth obtained with different codes/libraries in the CC6 layout

CR	Code	Library	C/E	C-E
CR1	SERPENT	JEFF3.1	0.915	$> 3\sigma$
	ERANOS		0.995	$< 1\sigma$
		ENDF/B-VI.8	1.019	$< 1\sigma$
	MCNP6.1	JEFF-3.2	0.880	$> 3\sigma$
CR2	SERPENT	JEFF3.1	0.929	$< 3\sigma$
	ERANOS		0.956	$< 3\sigma$
		ENDF/B-VI.8	0.979	$< 1\sigma$
	MCNP6.1	JEFF-3.2	0.893	$< 3\sigma$

Table 5C/E and C-E values for spectral indices obtained with different codes/libraries in the EFA-2 position of the CC6 layout

Spectral Index	Code	Library	C/E	C-E
F28/F25	SERPENT	JEFF-3.1	0.899	> 3 σ
	ERANOS		0.945	< 3 σ
		ENDF/B-VI.8	0.966	< 3 σ
	MCNP6.1	JEFF-3.2	0.937	< 3 σ
		ENDF/B-VII.1	0.918	> 3 σ
		TENDL-2014	0.928	< 3 σ
F49/F25	SERPENT	JEFF-3.1	0.999	< 1 σ
	ERANOS		1.011	< 1 σ
		ENDF/B-VI.8	1.010	< 1 σ
	MCNP6.1	JEFF-3.2	0.992	< 1 σ
		ENDF/B-VII.1	1.002	< 1 σ
		TENDL-2014	1.000	< 1 σ
F37/F25	SERPENT	JEFF-3.1	0.956	< 3 σ
	ERANOS		0.964	< 3 σ
		ENDF/B-VI.8	0.951	< 3 σ
	MCNP6.1	JEFF-3.2	0.920	< 3 σ
		ENDF/B-VII.1	0.953	< 3 σ
		TENDL-2014	0.952	< 3 σ

Table 6C/E values for the lead void reactivity effect obtained with different codes/libraries in the CC6 layout

Case	Code	Library	C/E	C-E
A	MCNP5	JEFF-3.1	0.978	$< 1\sigma$
	SERPENT		0.962	$< 1\sigma$
	ERANOS		1.244	$> 3\sigma$
		ENDF/B-VI.8	1.311	$> 3\sigma$
	MCNP6.1	JEFF-3.2	1.047	$< 1\sigma$
		ENDF/B-VII.1	1.007	$< 1\sigma$
B	MCNP5	JEFF-3.1	0.993	$< 1\sigma$
	SERPENT		1.007	$< 1\sigma$
	ERANOS		1.152	$> 3\sigma$
		ENDF/B-VI.8	1.181	$> 3\sigma$
	MCNP6.1	JEFF-3.2	1.067	$< 1\sigma$
		ENDF/B-VII.1	1.007	$< 1\sigma$

Table 7ERANOS / ENDF/B-VI.8 results of the uncertainty on the k_{eff} value summed over the 15 energy groups per each isotope considered and per each cross-section (pcm)

Isotope	Capture	Fission	ν	Elastic	Inelastic	n, xn	Total
^{56}Fe	36			6	40		54
^{208}Pb	14			5	24	2	29
^{207}Pb	43			2	16	1	46
^{206}Pb	57			3	23	1	62
^{52}Cr	5			4	3		8
^{235}U	2050	230	535	46	57	9	2130
^{238}U	173	34	114	15	189	7	282
^{27}Al	8			6	20		22
^{16}O	61			23	7		66
Total	2060	232	547	50	206	12	**2150**

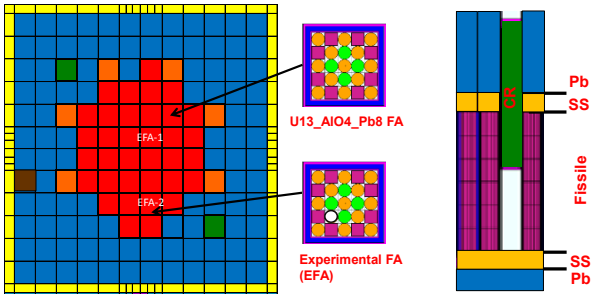

Fig. 1 The VENUS-F CC5 layout (left frame), the standard FA and the EFA (central frame), an axial view of some FAs with a partially inserted CR (right frame). The CC5 layout is made of 33 FAs (red), 2 EFAs (red), 6 fuel follower SRs (orange), 2 CRs (dark green), 1 POAR rod (brown), the surrounding LAs (blue) and SS casing (yellow). The FA is made of 13 U rods (orange), 8 lead blocks (purple), 4 Al_2O_3 rods (light green) and a SS-Pb casing (magenta-blue).

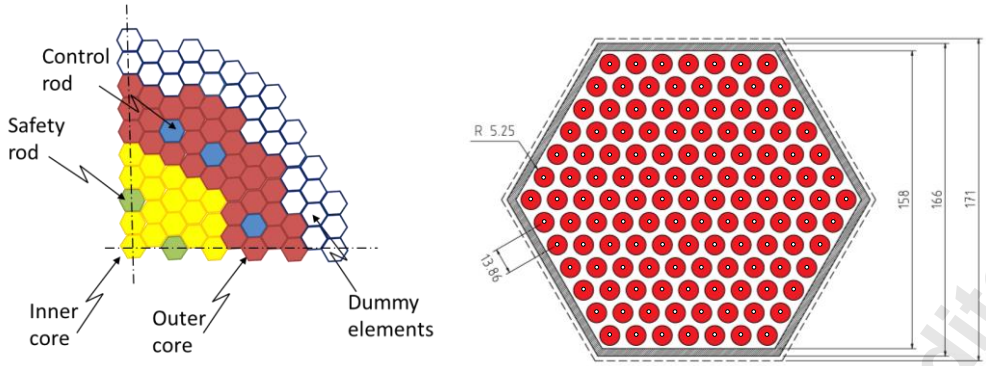

Fig. 2 The ALFRED LFR core layout (1/4 symmetry, left frame) and FA design (right frame) [4]

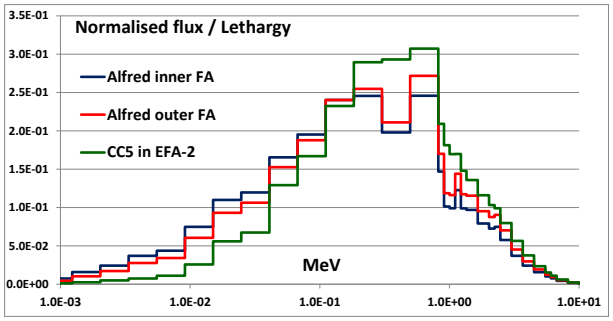

Fig. 3 Comparison between neutron spectra calculated in the CC5 layout (EFA-2 position, core mid-plane) and in the ALFRED inner and outer FAs (ERANOS/JEFF-3.1, semi-logarithmic scale)

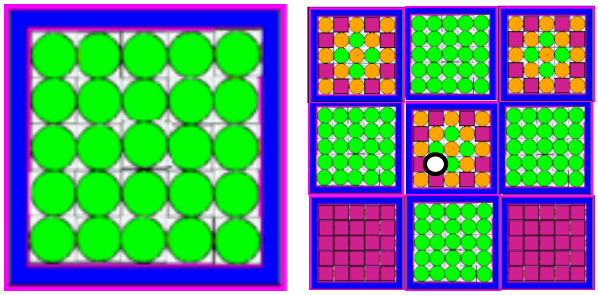

Fig. 4 The AIA (left frame, made of 25 Al_2O_3 rods) and the 3x3 ALFRED island (right frame) made of: 4 AIAs, 2 standard FAs, 2 LAs and the EFA-2 in the center

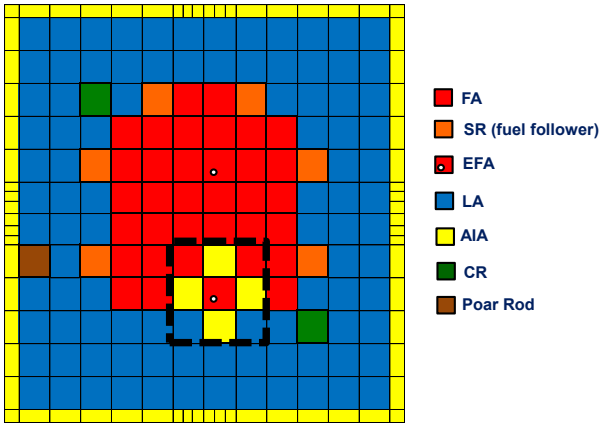

Fig. 5 The VENUS-F CC6 layout representative of ALFRED made of: 33 FAs, 6 fuel follower SRs, 2 EFAs, 4 AIAs, 2 CRs, 1 POAR rod, the surrounding LAs and SS casing.

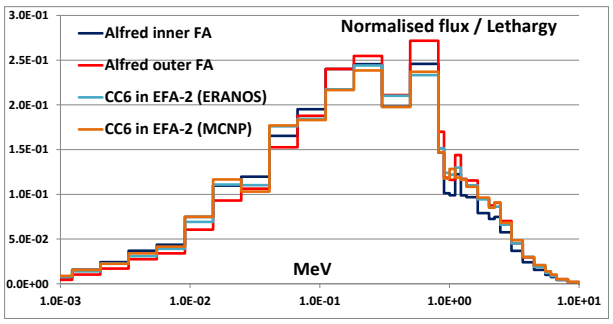

Fig. 6 Calculated spectra in the CC6 layout (EFA-2 position, core mid-plane) compared with the ALFRED FA ones (ERANOS/JEFF-3.1 and MCNP6.1/JEFF-3.2; semi-logarithmic scale)

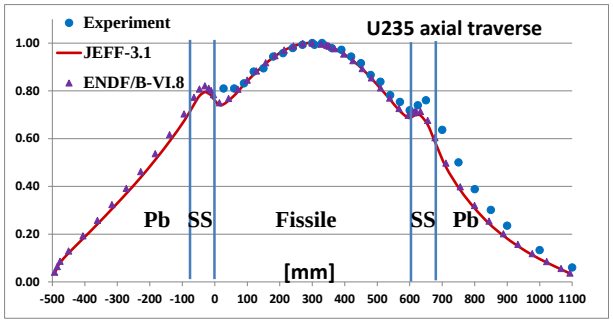

Fig. 7 Experimental and ERANOS (JEFF-3.1 and ENDF/B-VI.8) axial traverses in EFA-2 for U^{235} fission rates (normalized to 1 at core mid-plane)

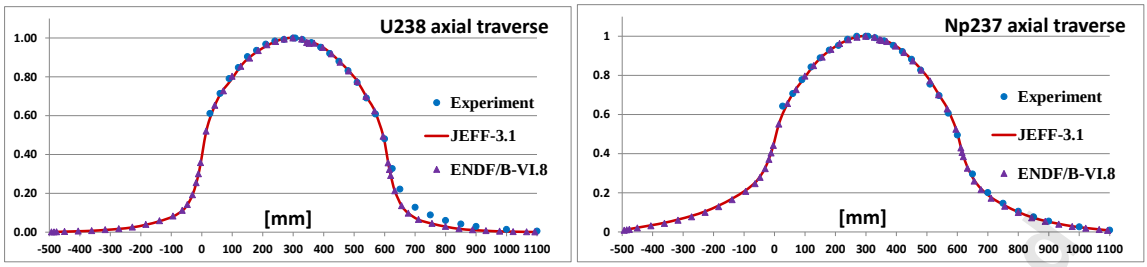

Fig. 8 Experimental and ERANOS (JEFF-3.1 and ENDF/B-VI.8) axial traverses in EFA-2 for U^{238} (left) and Np^{237} (right) fission rates (normalized to 1 at core mid-plane)

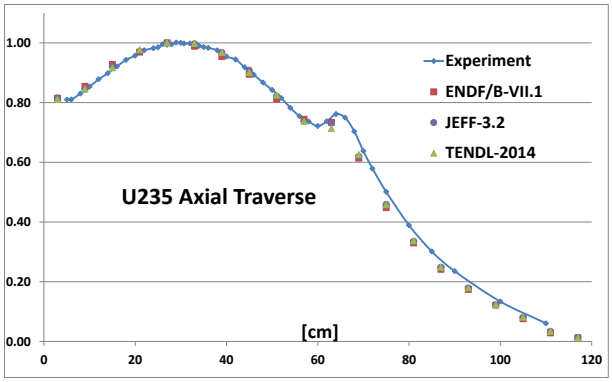

Fig. 9 Experimental and MCNP6.1 (JEFF-3.2, ENDF/B-VII.1 and TENDL-2014) axial traverses in EFA-2 for U^{235} fission rates (normalized to 1 at core mid-plane)

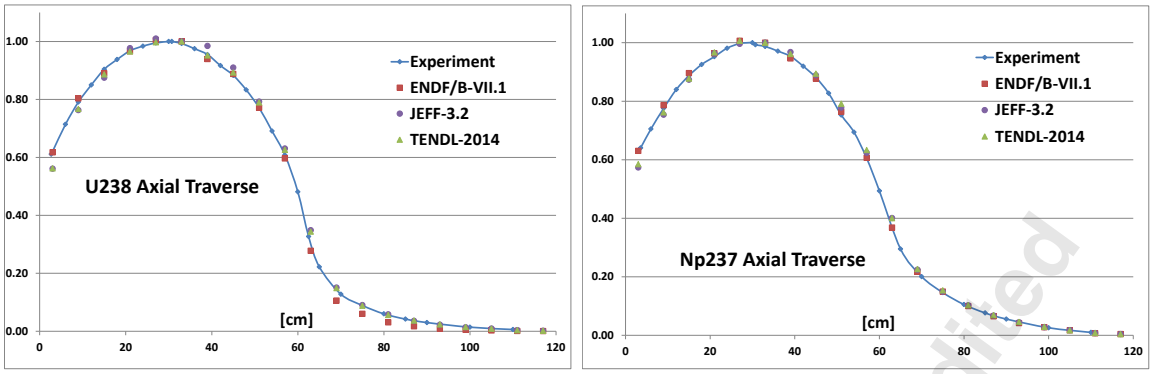

Fig. 10 Experimental and MCNP6.1 (JEFF-3.2, ENDF/B-VII.1 and TENDL-2014) axial traverses in EFA-2 for U^{238} (left) and Np^{237} (right) fission rates (normalized to 1 at core mid-plane)

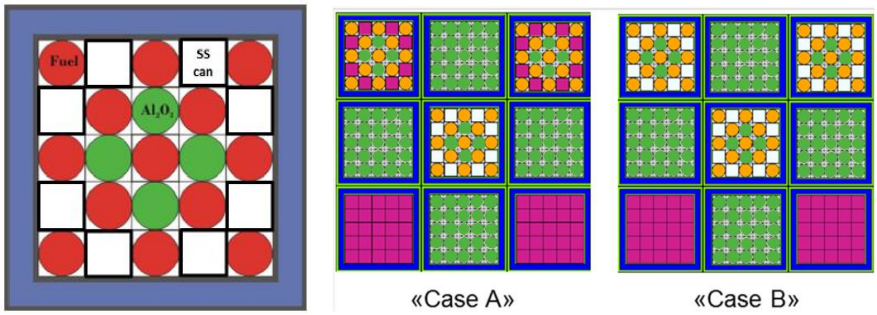

Fig. 11 Voided FA (left frame); Cases A and B measured and simulated with one and three FAs voided, respectively (right frame)

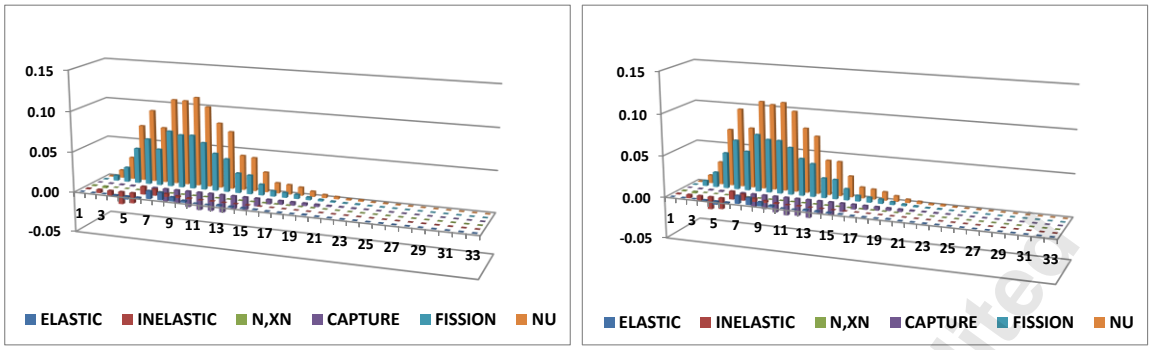

Fig. 12 ERANOS / JEFF-3.1 (left) and ERANOS / ENDF/B-VI.8 (right) values of the sensitivity coefficients summed over the isotopes per each energy group and per each cross-section

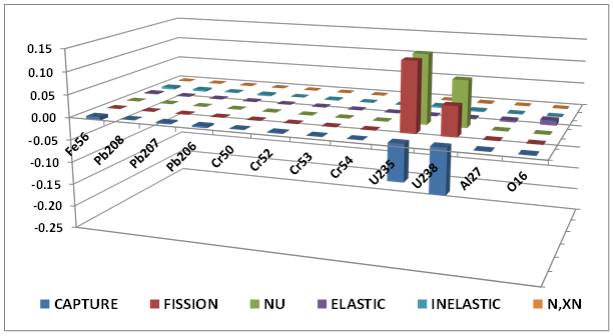

Fig. 13 ERANOS / JEFF-3.1 values of the sensitivity coefficients summed over the 33 energy groups per each isotope and per each cross-section

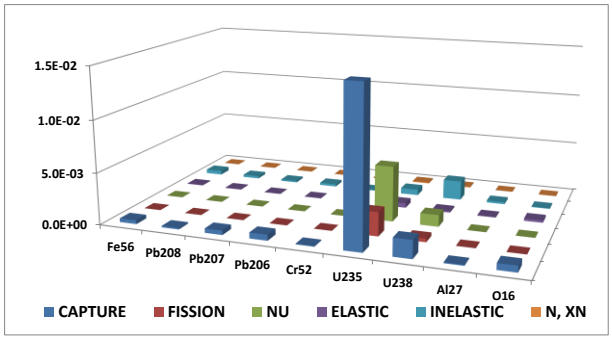

Fig. 14 ERANOS-ENDF/B-VI.8 results of the uncertainty on the k_{eff} value summed over the 15 energy groups per each isotope and per each cross-section

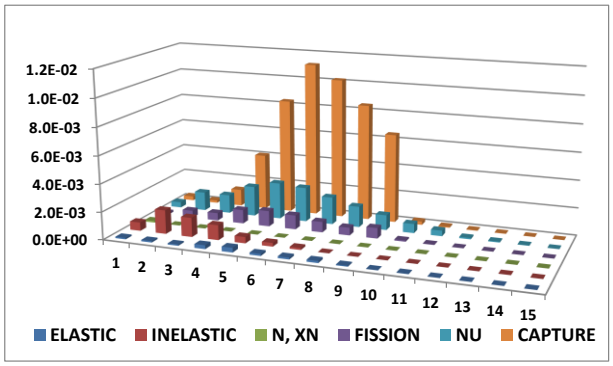

Fig. 15 ERANOS-JEFF3.1 results of the uncertainty on the k_{eff} value summed over the isotopes per each energy group and per each cross-section